JPET Fast Forward. Published on March 15, 2005 as DOI: 10.1124/jpet.104.079616

LONG-TERM TREATMENT OF BILE DUCT LIGATED RATS WITH RAPAMYCIN (SIROLIMUS) SIGNIFICANTLY ATTENUATES LIVER FIBROSIS: ANALYSIS OF THE UNDERLYING MECHANISMS

Erwin Biecker, Andrea De Gottardi, Markus Neef, Matthias Unternährer, Vreni Schneider, Monika Ledermann, Hans Sägesser, Sidney Shaw and Jürg Reichen

Department of Clinical Pharmacology
University of Berne
Murtenstrasse 35
3010 Berne
Switzerland
(EB, AdG, MN, MU, VS, ML, HS, JR)

Department of Clinical Research
University of Berne
Murtenstrasse 35
3010 Berne
Switzerland
(SS)

Running title page:

Running title: Sirolimus and liver fibrosis

Author for correspondence:
Jürg Reichen, MD
Department of Clinical Pharmacology
University of Berne
Murtenstrasse 35
3010 Berne, Switzerland
Tel. 0041 31 632 8711
Fax 0041 31 632 4997
Email: reichen@ikp.unibe.ch

Number of text pages: 36

Number of tables: 5

Number of figures: 8

Number of references: 46

Word count abstract: 246

Word count introduction: 563

Word count discussion: 1499

Section assignment: Gastrointestinal and hepatic

Abbreviations: 4E-BP1: eukaryotic initiation factor 4E-binding protein, BDL: bile duct ligation, BDL CTR: BDL rats without rapamycin treatment, BDL SIR: BDL rats with rapamycin treatment, CAB: Chromotrop-Anilinblue trichrome, CTGF: connective tissue growth factor, eIF: eukaryotic initiation factor, FKBP: FK binding protein, HEK: human embryonic kidney, HSC: hepatic stellate cell, MAP: mean arterial pressure, mTOR: mammalian target of rapamycin, NRC: normal rat cholangiocyte, p21; cyclin dependent kinase inhibitor $p21^{WAF1/CIP1}$, p27: cyclin dependent kinase inhibitor $p27^{kip}$, p-4E-BP1:

JPET Fast Forward. Published on March 15, 2005 as DOI: 10.1124/jpet.104.079616
This article has not been copyedited and formatted. The final version may differ from this version.

phosphorylated 4E-BP1, $p70^{s6k}$: p70 S6 kinase, PDGF: platelet derived growth factor, PI3K: Phosphoinositide-3-kinase, p-$p70^{s6k}$: phosphorylated $p70^{s6k}$, pRb: retinoblastoma protein, PVP: portal venous pressure, SMA: smooth muscle actin

Abstract:

Background: Rapamycin is an immunosuppressant with anti-proliferative properties. We investigated whether rapamycin treatment of bile duct ligated (BDL) rats is capable to inhibit liver fibrosis and thereby affect hemodynamics. Methods: Following BDL, rats were treated for 28 days with rapamycin (BDL SIR). BDL animals without drug treatment (BDL CTR) and sham-operated animals served as controls. After 28days, hemodynamics were measured and livers were harvested for histology/immunohistochemistry. Liver mRNA levels of transforming growth factor (TGF)-β1, connective tissue growth factor (CTGF), platelet derived growth factor (PDGF) beta, p27 and p21 were quantified by rtPCR. Liver protein levels of p27, p21, $p70^{s6k}$, phospho-$p70^{s6k}$, 4E-BP1, phospho-4E-BP1(Thr37/46) and phospho-4E-BP1(Ser65/Thr70) were determined by Western blotting. Results: Portal vein pressure was lower in BDL SIR than in BDL CTR animals. Volume fractions of connective tissue, bile duct epithelial, desmin-positive and actin-positive cells were lower in BDL SIR than in BDL CTR rats. On the mRNA level, TGF-β1, CTGF and PDGF were decreased by rapamycin. p27 and p21 mRNA did not differ. On the protein level, rapamycin increased p27 and decreased p21 levels. Levels of non-phosphorylated $p70^{s6k}$ and 4E-BP1 did not vary between groups but levels of p-$p70^{s6k}$ were decreased by rapamycin. Rapamycin had no effect on p-4E-BP1(Thr37/46) and p-4E-BP1(Ser65/Thr70) levels. Conclusions: In BDL rats, rapamycin inhibits liver fibrosis and ameliorates portal hypertension. This is paralled by decreased levels of TGF-β1, CTGF and PDGF. Rapamycin influences the cell cycle by upregulation of p27, downregulation of p21 and inhibition of $p70^{s6k}$ phosphorylation.

Introduction:

Induction of secondary biliary cirrhosis by bile duct ligation is a widely used and accepted model to study the pathophysiological changes that take place during the development of hepatic fibrosis and portal hypertension. Four weeks after bile duct ligation, secondary biliary cirrhosis with a decrease in functional parenchyma, an increase in fibrosis and proliferation of bile ducts is fully established(Zimmermann et al., 1994). These histological and structural changes are paralleled by the development of portal hypertension, porto-systemic shunts and the hyperdynamic circulation syndrome(Van de Casteele et al., 2001), which is characterized by a decrease in systemic vascular resistance and an increase in cardiac output. Hepatic stellate cells (HSC) are the key players in the development of fibrosis following liver injury. Upon injury, the cells undergo activation and transformation into myofibroblasts and become proliferative and fibrogenic. The most potent mitogen for HSC is platelet derived growth factor (PDGF)(Pinzani et al., 1991). PDGF is secreted in an autocrine fashion by HSC but is also synthesized by cholangiocytes during cholestasis(Grappone et al., 1999). Transforming growth factor (TGF) β1 is the most important fibrogenic stimulus for HSC(Friedman, 1999). TGF-β1 levels are increased in liver fibrosis and regulate HSC activity in an autocrine mode. Another important cytokine that is involved in fibrogenesis is connective tissue growth factor (CTGF). CTGF is a down-stream mediator of TGF-β1, mediating and potentiating some of the effects of TGF-β1 like fibroblast proliferation and extracellular matrix production(Frazier et al., 1996) through a not yet defined receptor.

The macrolide fungicide rapamycin, also known as sirolimus, was initially introduced into clinical practice as an immunosuppressive drug. In addition, it possesses potent antimicrobial and anti-proliferative properties. The anti-proliferative action of rapamycin is due to the ability to interfere with cell cycle progression in response to proliferative stimuli(Wiederrecht et al., 1995). Rapamycin binds intracellularly to FK506 binding proteins

(FKBPs). The most important binding protein regarding the rapamycin-sensitive pathway is FKBP12(Fruman et al., 1995). The complex of FKBP12 and rapamycin inhibits the mammalian target of rapamycin (mTOR)(Sabatini et al., 1994). It belongs to the family of phosphoinositide 3-kinase related kinases (PIKKs) and is involved in the control of crucial growth-related cellular functions. mTOR is not part of a common linear signaling pathway. Signaling through mTOR is activated by the presence of sufficient nutrients (mainly amino acids) and phosphoinositide 3-kinase (PI3K) signaling. However, it is not clear yet, whether PI3K directly regulates mTOR or if the two pathways function independently.

mTOR activates the 40S ribosomal protein S6 kinase ($p70^{s6k}$) and inhibits the eukaryotic initiation factor (eIF) 4E binding protein-1 (4E-BP1)(Gingras et al., 1998) by phosphorylation, thus enabling the assembly of the eIF4F complex. The second downstream mediator of mTOR, $p70^{s6k}$, phosphorylates the 40S ribosomal protein S6 and thereby enhances the translation of mRNA of proteins essential for cell cycle progression. In addition, rapamycin decreases the concentration of cyclin D1 and thereby decreases retinoblastoma protein (pRb) phosphorylation(Morice et al., 1993), blocks the elimination of the cyclin dependent kinase inhibitor p27(Nourse et al., 1994) and inhibits expression of p21, another cyclin dependent kinase inhibitor(Gaben et al., 2004).

It is the purpose of the present study to investigate the impact of rapamycin on liver fibrosis and on the hemodynamics in bile duct ligated (BDL) rats. In addition, the effect of rapamycin on pro-fibrogenic and/or pro-mitogenic cytokines like TGF-β1, CTGF and PDGF and on cell-cycle regulatory proteins regulated by mTOR is studied.

JPET Fast Forward. Published on March 15, 2005 as DOI: 10.1124/jpet.104.079616
This article has not been copyedited and formatted. The final version may differ from this version.

Methods:

Animals, induction of cirrhosis, medical treatment:

Male Wistar rats were kept under a 12 hour light-dark cycle with free access to rat chow (Kliba, Kaiseraugst, Switzerland) and water. The animal experiments had been approved by a state-appointed board on animal ethics and were performed according to international guidelines concerning the conduct of animal experimentation.

To induce biliary cirrhosis, animals underwent double ligation and section of the common bile duct (BDL) under pentobarbital anesthesia (50 mg/kg intraperitoneally). In addition, six animals were sham-operated(Gross et al., 1987).

The rats were divided into three groups: BDL animals in the treatment group (BDL SIR) were treated with 2.0 mg/kg/d of rapamycin (Rapamune®, Wyeth/AHP, Zug, Switzerland) in the drinking water, BDL animals in the non-treatment group which received no drug treatment (BDL CTR) and sham-operated animals which received no drug treatment. Treatment for 28 days was started immediately after BDL.

Hemodynamic measurements and tissue conservation:

Hemodynamic measurements were performed under pentobarbital anesthesia (50 mg/kg, intraperitoneally). A femoral artery and vein as well as a carotid artery were cannulated with a PE-50 tube (Parsippany, New York, USA). Then, the abdomen was opened and a PE-50 tube (Parsippany) was introduced into the portal via an ileocolic vein. Portal vein pressure and mean arterial pressure were measured using Statham transducers (Braun, Melsungen, Germany). Cardiac output and organ blood flow were determined using the microsphere technique(Groszmann et al., 1982): The catheter in the carotid artery was advanced into the left ventricle, ^{113}Tn-labeled microspheres were injected and the reference sample was withdrawn using a Harvard infusion pump set to 1ml/min. Portosystemic shunting

was determined by injection of ^{57}Co-labeled microspheres into the portal vein. Then rats were killed by exsanguination, while taking blood samples for analyzing activity of AST, alkaline phosphatase, serum levels of the drug, bile acids and TGF-β1 immunoassay. The visceral organs were removed and weighed. The liver was cut into pieces. Liver samples were either snap-frozen in liquid nitrogen and stored at –75 °C for Western blotting, put into Tissue-Tek (Sakura, Netherlands) and stored at –20 °C for immunohistochemistry, put into RNAlater (Ambion, Huntingdon, UK) for RNA extraction or stored in formaldehyde for histology. The remaining part of the liver was used for gamma counting. The γ-isotopes in organs were measured on a Packard COBRA-II γ-spectrophotometer (Perkin Elmer, Hünenberg, Switzerland) with appropriate corrections for isotope spillover. Organ flow and porto-systemic shunting was calculated as described by Groszman and Co-workers(Groszmann et al., 1982).

RNA isolation and purification:

At least five randomly chosen samples from different regions of the liver with a total of 100 mg of tissue were taken and put into 1 ml of Trizol (Invitrogen, Basel, Switzerland). The samples were disrupted and homogenized in Trizol using a MM 300 vibration mill (Retsch, Haan, Germany) and RNA was extracted following the manufacturer's guidelines. RNA concentration was measured spectrophotometrically using a Genequant Pro (Amersham Biosciences, Dübendorf, Switzerland) instrument.

DNA digestion and reverse transcription:

5 µg total RNA were used of each liver sample. Prior to reverse transcription, samples were DNA digested by incubation with RQ1 RNase-free DNase (Promega, Wallisellen, Switzerland). Reverse transcription was done using Moloney Murine Leukemia Virus reverse transcriptase (Invitrogen) and random primers (250 ng, Microsynth, Balgach, Switzerland). Control reactions did not contain reverse transcriptase.

JPET Fast Forward. Published on March 15, 2005 as DOI: 10.1124/jpet.104.079616
This article has not been copyedited and formatted. The final version may differ from this version.

Quantitative real-time PCR:

Primers and probes were designed using the Primer Express Software (Applied Biosystems, Rotkreuz, Switzerland) and custom synthesized by Microsynth or Applied Biosystems, respectively. Sequences and Genebank accession numbers of the primers and probes (except for p21 which was bought as an "assay on demand" from Applied Biosystems) are given in detail in Table 1.

Real-time PCR was performed using the ABI 7700 Sequence detector (Applied Biosystems) as described and referenced before(Biecker et al., 2004). A dual-labeled fluorogenic probe (labeled with a „reporter" dye at the 5'-end and a second dye, quenching the emission of the „reporter" dye at the 3'-end) complementary to a sequence within each PCR product was added to the PCR reaction. Cleavage of the probe during elongation by the exonuclease activity of the Taq DNA polymerase separates the reporter from its quencher. Accumulation of PCR products is detected real-time by monitoring the increase in fluorescence of the reporter dye. The PCR reaction was performed in a volume of 25 µl containing 12.5 µl 2x TaqMan PCR master mix (Applied Biosystems) as well as 1.2 µl (equivalent to 300 ng total RNA) cDNA. The concentrations of the primers and probes are given in table 1. Glyceraldehyde 3-phosphate dehydrogenase (GAPDH) provided as „ready-to-use" primers (100 nmol/l each) and probe (200 nmol/l) by the manufacturer (rodent GAPDH endogenous control, Applied Biosystems) served as the endogenous control.

The results were expressed as the number of cycles (C_T value) at which the fluorescence signal exceeded a defined threshold. The difference in C_T values of the target cDNA and the endogenous control (GAPDH) are expressed as ΔC_T values. Therefore, lower ΔC_T values denote higher mRNA levels. The $\Delta\Delta C_T$-method was used for quantification of the results. For all the used sets of primers and probes, a validation experiment was performed according to the manufacturers guidelines. It was demonstrated in those experiments, that the efficiencies

of the real-time PCR for the target and reference were approximately equal and the $\Delta\Delta C_T$-method could therefore be used for relative quantification.

TGF-β1 immunoassay:

Plasma samples of six animals of each group were taken and analyzed using a Quantikine TGF-β1 immunoassay (R&D Systems, Wiesbaden, Germany) following the manufacturer's guidelines. Results were calculated by construction of a standard curve by plotting the mean absorbance for each standard on the y-axis against the concentration on the x-axis and drawing of a best fit curve through the points on the graph. The data was then linearized by plotting the log of the TGF-β1 concentrations versus the log of the O.D. and the best fit line was determined by regression analysis.

Western Blot analysis:

At least five randomly chosen samples from different regions of the liver with a total of 500 mg of tissue were taken from each organ and put into 2 ml of 0.25 mol/l sucrose buffer containing a mixture of proteinase-inhibitors (complete mini tablets, Roche, Mannheim, Germany) at 4 °C and homogenized using a MM 300 vibration mill (Retsch). Samples were then centrifuged for 10 min at 12000 g to remove cell debris. The supernatant was used in the subsequent experiments. Protein concentration was measured according to Lowry(Lowry et al., 1951). Proteins from whole liver homogenate were separated by sodium-dodecyl sulfate-polyacrylamide gel (SDS-PAGE) electrophoresis and subsequently transferred to nitrocellulose membranes (Schleicher und Schüll, Dassel, Germany). The membranes were blocked with 5% non-fat dry-milk in incubation buffer at 4°C overnight and probed for 2 hours with the primary antibodies at room-temperature. The membranes were washed three times, incubated at room-temperature for 1 hour with peroxidase-conjugated secondary antibody, washed three times and the signal was revealed by enhanced chemiluminescence (Western Lightning chemiluminescence reagent, Perkin Elmer). The data of the antibodies and conditions are given in detail in table 2. Protein extracts of HEK cells harvested in the

exponential growing phase served as positive controls. Intensity of antigenic signals was videoimaged (FujiFilm LAS-1000, FujiFilm, Düsseldorf, Germany) and quantified by using a software package (AIDA, Raytest, Urdorf, Switzerland). Densitometric integrated values (area of the band x density of the band) were determined and the results expressed as arbitrary units.

Immunohistochemistry:

Immunohistochemistry for desmin and α-smooth muscle actin (SMA) was performed on one (per animal) randomly selected piece of rat liver as described before by this laboratory(Tieche et al., 2001). In brief, desmin was demonstrated by a mouse-anti-desmin monoclonal antibody (clone D33, Dako, Glostrup, Denmark) at a concentration of 5.3 μg/ml and an incubation time of 60 min. Following the washing steps, a rabbit-anti-mouse IgG antibody, absorbed with rat serum (Dako), diluted 1:50, served as the link antibody to the alkaline phosphatase-anti-alkaline phosphatase (APAAP) mouse monoclonal antibody (Dako; 1:50 in TBS, 45 min) that was applied as the third layer. SMA was detected using a mouse-anti-SMA (clone 1A4, Sigma), 1:600 in TBS for 60 min. After the primary antibody, a biotinylated rabbit-anti-mouse IgG antibody, absorbed with rat serum (Dako) was applied (1:200, 45 min), followed by a streptavidin-biotin complex/alkaline phosphatase system (Dako), 1:200, 45 min. Finally, slides were developed in new fuchsin-naphtol AS-BI (Sigma), counterstained with hematoxylin, and mounted.

CAB-staining:

Three (per animal) randomly selected pieces of rat liver were fixed in neutrally buffered formaldehyde 4% and embedded in paraffin. 2-3 μm sections were deparaffinized and fixed in Bouin's solution (saturated picrinic acid, 40% formaldehyde, 98% acetic acid, 15:5:1). Cellular nuclei were visualized using Weigert's ferrum-hematoxylin. After incubation with 1% phosphomolybdenic acid, the sections were stained by chromotrope-anilin blue.

Morphometry:

To estimate the volumetric density of different tissue components, a point counting procedure was carried out on liver sections using a microscope with a sampling stage, connected to a semiautomatic advancer(Gross et al., 1987). In CAB-stained sections, 1500 points per animal were counted and each of them classified overlying either hepatocyte, bile duct epithelial cell or connective tissue.

Immunohistochemistry was used to distinguish hepatic stellate cells (desmin positive) from their activated counterparts expressing α-smooth muscle actin(Tieche et al., 2001). 500 points per animal were counted and hepatic stellate cells further classified as either portal/septal or parenchymal (surrounded by hepatocytes). Results are presented as volume fraction (percentage of specific cells over total number of counted cells).

Statistical analysis:

The three groups (sham-operated rats, BDL rats with rapamycin treatment and BDL rats without treatment) were compared by ANOVA / Bonferroni/Dunn procedure for multiple testing (StatView 5.0, SAS Institute Inc., Cary, NC, USA). The alpha-value was set to 5% and a $p < 0.0167$ was considered statistically significant. Morphometric analysis was done in two groups (BDL rats with rapamycin treatment and BDL rats without treatment) only. In this case a $p<0.05$ was considered statistically significant.

JPET Fast Forward. Published on March 15, 2005 as DOI: 10.1124/jpet.104.079616
This article has not been copyedited and formatted. The final version may differ from this version.

Results:

Animal characterization:

Table 3 shows the animal characteristics. The body weight of BDL CTR rats was significantly higher than the body weight of the sham-operated animals. No significant differences were obtained comparing BDL SIR rats with sham-operated animals and with BDL CTR animals. Liver weight was highest in the BDL CTR group, followed by the BDL SIR rats and was lowest in the sham-operated animals ($p<0.001$ between all groups). Spleen weight of the sham animals and of BDL SIR rats did not vary significantly but was significantly higher in the BDL CTR animals ($p<0.001$). These results demonstrate that rapamycin treatment attenuates the increase in liver weight that typically succeeds BDL. Furthermore, the normal spleen weight in the BDL SIR rats is an indicator for the absence of portal hypertension. The laboratory values for AST, bilirubin and bile acids reflect the positive effect of the rapamycin treatment. AST, bilirubin and bile acids were markedly elevated in the BDL CTR group ($p<0.01$ compared to BDL SIR and sham-operated rats) whereas values for BDL SIR and sham-operated animals did not differ significantly.

Hemodynamic studies:

As it was already indicated by the normal spleen weight, the hemodynamic parameters (table 4) were favorably influenced by the rapamycin treatment. MAP was not significantly different between groups but showed a tendency for higher pressure in the BDL SIR compared to BDL CTR animals. Portal venous pressure was highest in the BDL CTR rats, lower in the BDL SIR animals and was lowest in the sham-operated rats ($p<0.01$ between all groups). Cardiac output was higher in the BDL CTR rats than in BDL SIR rats and in sham-operated animals. However, only the difference between sham-operated animals and BDL SIR rats was statistically significant ($p<0.05$). Hepatic artery blood flow was significantly

JPET Fast Forward. Published on March 15, 2005 as DOI: 10.1124/jpet.104.079616
This article has not been copyedited and formatted. The final version may differ from this version.

lower in BDL SIR animals than in sham-operated or BDL CTR rats ($p<0.001$). Portal vein blood flow was highest in sham-operated animals and only slightly lower in BDL SIR animals. Lowest values were obtained in BDL CTR rats ($p=0.01$ comparing BDL CTR animals with BDL SIR rats and $p<0.001$ comparing BDL CTR rats with sham-operated animals).

Morphometry:

To prove that the positive effect of the rapamycin treatment on the hemodynamic parameters was paralleled by an inhibition of the histological changes that follow BDL, we performed microscopic examination and morphometry (figure 1 and table 5) of liver sections. The BDL SIR group had a significantly higher volume fraction of hepatocytes compared to the BDL CTR group. In contrast, the volume fractions of connective tissue, bile duct epithelial cells, desmin positive and actin positive cells were significantly lower in the BDL SIR group than in the BDL CTR group. The comparison of actin positive cells to desmin positive cells gave mean fractions of 0.34 in the BDL SIR group and 0.71 in the BDL CTR group.

Growth factors:

As we were able to show that long-term treatment of BDL rats with rapamycin blocks the development of fibrosis as well as bile duct proliferation, we studied the underlying mechanisms. In a first step, we investigated the liver mRNA steady-state levels of the most important pro-fibrogenic and pro-mitogenic factors. Figure 2a shows the results of the quantitative PCR for TGF-β1. Compared to sham-operated animals, BDL CTR rats exhibited a 5.0-fold increase ($p<0.001$) while BDL SIR rats exhibited only a 2.5-fold ($p<0.05$) increase in TGF-β1 mRNA steady state levels. This inhibitory effect on the mRNA expression was paralleled by an inhibitory effect of rapamycin treatment on TGF-β1 plasma levels (figure 3).

JPET Fast Forward. Published on March 15, 2005 as DOI: 10.1124/jpet.104.079616
This article has not been copyedited and formatted. The final version may differ from this version.

Compared to BDL CTR rats, rapamycin treatment did decrease TGF-β1 plasma levels by 20%.

Liver CTGF mRNA steady-state levels (Figure 2b) were massively increased by BDL (86.8-fold increase compared to sham-operated animals, $p<0.001$) whereas BDL SIR animals showed only an increase by a factor of 11.4 compared to sham-operated animals ($p<0.001$; $p<0.001$ comparing BDL CTR with BDL SIR animals).

Liver PDGF beta chain mRNA steady state levels (Figure 2c) were increased by BDL by a factor of 29.2 ($p<0.001$). BDL SIR rats showed an increase by a factor of 8.8 compared to sham-operated rats ($p<0.001$; $p<0.01$ comparing BDL CTR with BDL SIR animals).

These results clearly show that rapamycin treatment inhibits the gene expression of the most important pro-fibrogenic and pro-mitogenic cytokines. However, a complete normalization to the levels of the sham-operated animals was not achieved.

Cell-cycle regulatory proteins:

In addition to the effect on growth factors, rapamycin is known to have a direct inhibitory effect on the cell-cycle machinery. Therefore, we studied the effect of rapamycin treatment on the most important cell-cycle regulatory proteins that are known to be affected by rapamycin. Figure 4a shows the mRNA steady-state levels of the cyclin dependent kinase inhibitor p27 in the liver. Neither BDL alone nor BDL and rapamycin treatment caused significant changes in the p27 mRNA levels. The protein levels of p27 are given in Figure 4b. In contrast to the findings on the mRNA level, significant differences were obtained on the protein level. Lowest levels were found in BDL CTR rats. Rapamycin treatment induced a significant increase in the p27 level but did not reach the p27 level of sham-operated animals ($p<0.01$ between all groups).

Next, liver mRNA and protein levels of the cyclin dependent kinase inhibitor p21 were studied (figure 5). Similar to the findings for p27, neither BDL nor BDL and rapamycin

treatment did significantly alter the mRNA steady state levels (Figure 5a). On the protein level (Figure 5b), significant differences were obtained ($p<0.01$ between BDL CTR and BDL SIR and sham-operated animals) with highest levels in BDL CTR animals. Rapamycin treatment caused a significant decrease of p21 protein levels in BDL SIR animals compared to BDL CTR animals but did not reach the p21 level of sham-operated animals.

The activity of 4E-BP1 is regulated by phosphorylation and dephosphorylation of the phosphorylation sites Thr37/46 and Ser65/Thr70. Figure 6 shows the liver protein levels of non-phosphorylated 4E-BP1, phospho-4E-BP1 (Thr37/46) and phospho-4E-BP1 (Ser65/Thr70). Protein levels of total, non-phosphorylated 4E-BP1 did not differ between the treatment groups. Similarly, protein levels of p-4E-BP1 (Thr37/46) did not vary significantly between groups. In contrast, we found significantly lower protein levels of p-4E-BP1 (Ser65/Thr70) in BDL CTR rats compared to sham-operated animals ($p<0.01$) but p-4E-BP1 (Ser65/Thr70) levels of BDL SIR rats did not differ significantly from BDL CTR animals or sham-operated rats. These results are in contrast to the documented effect of rapamycin on 4E-BP1 phosphorylation in cell culture models, since we were not able to show an effect on 4E-BP1 phosphorylation *in vivo*.

As it is the case for 4E-BP1, the activity of $p70^{s6k}$ is regulated by phosphorylation and dephosphorylation. It is shown in figure 7 that rapamycin treatment of BDL rats lowered phospho-$p70^{s6k}$ significantly ($p<0.001$). Furthermore, p-$p70^{s6k}$ levels in BDL CTR rats were significantly lower than in sham-operated animals ($p<0.01$; $p<0.01$ comparing sham-operated and BDL CTR rats). To prove that the increase in p-$p70^{s6k}$ is not due to a relative increased expression of total, non-phosphorylated $p70^{s6k}$ we used an antibody against total, non-phosphorylated $p70^{s6k}$ and did not find a difference between groups.

We were not able to detect pRb in the livers of BDL CTR, BDL SIR or sham-operated animals by Western blot analysis (figure 8). However, we found a strong signal in cultured human embryonic kidney (HEK) cells and in cultured normal rat cholangiocytes (NRC),

which were harvested in the exponential growing phase. Serum deprived (24 h) NRC cells showed a weaker band, whereas HEK cells, which were kept without serum for 96 h, displayed no band.

JPET Fast Forward. Published on March 15, 2005 as DOI: 10.1124/jpet.104.079616
This article has not been copyedited and formatted. The final version may differ from this version.

Discussion

Prevention of liver fibrosis by rapamycin was first demonstrated in rats exposed to long-term treatment with CCl_4 by Zhu (Zhu et al., 1999). We expand this observation in another model and also demonstrate amelioration of hemodynamic changes, inhibition of bile duct proliferation and finally, the signal transduction pathway of the antifibrotic effects of rapamycin.

Rapamycin treatment of rats started immediately after bile duct ligation significantly inhibits the development of liver fibrosis as evidenced by a decrease in the volume fraction of connective tissue and of activated hepatic stellate cells. Activation of HSC is mediated predominantly by PDGF, TGF-β1 and its down-stream mediator CTGF. All three cytokines were markedly upregulated in BDL and reduced by a factor of 2 to 8 by rapamycin. PDGF, the most potent proliferative factor for HSC is synthesized not only by HSC but also by cholangiocytes during cholestasis(Grappone et al., 1999). The cytokine is a dimer composed of PDGF-A or –B with the three possible isoforms AA, BB or AB. PDGF BB is the most potent form in stimulating HSC proliferation; mRNA steady-state levels of the B-chain in the liver was decreased by a factor of three by rapamycin.

The expression of TGF-β1 mRNA - thought to be the major stimulus for fibrogenesis in HSC (Friedman, 1999) – was decreased by half by rapamycin treatment. The reduced expression of TGF-β1 mRNA in rapamycin treated animals was paralled by only a minor decrease in TGF-β1 plasma levels; this is due to the predominantly auto- and paracrine action of TGF-β1. Our results are in line with a suppression of TGF-β1 secretion in an immortalized human HSC line (Shibata et al., 2003) and the decreased TGF-β1 mRNA levels in the liver of rapamycin treated rats (Zhu et al., 1999). However, our results are in contrast to the findings of other authors who described an increase in TGF-β1 mRNA and/or plasma levels by rapamycin in the plasma of human kidney transplant recipients (Khanna et al., 2002), human

lymphocytes (Khanna, 2000), transformed and non-transformed cultured cells (Law et al., 2002), rat kidney (Shihab et al., 2004) and prostate cancer cells (van der Poel, 2004). As these experiments were not conducted using either hepatocytes or HSC, we conclude that the effect of rapamycin in the liver might differ from the effect in other tissues.

The most dramatic effect was seen in the message of CTGF, a downstream mediator of TGF-β (Moussad and Brigstock, 2000) involved in experimental and human liver cirrhosis (Paradis et al., 1999; Williams et al., 2000). CTGF is produced in HSC (Paradis et al., 1999; Williams et al., 2000) and proliferating cholangiocytes (Sedlaczek et al., 2001). Both, cholangiocytes and activated HSC were markedly reduced by rapamycin treatment. Further studies will be needed to delineate which cell type is mostly responsible for the decrease in fibrogenic cytokines.

The hemodynamic changes induced by bile duct ligation in rats are favorably influenced by rapamycin treatment as shown by a decrease in portal pressure and an increase in portal blood flow. Interestingly, hepatic artery blood flow was significantly lower in BDL SIR compared to both BDL CTR and sham rats. An increase in hepatic arterial blood flow is seen in different models of portal hypertension, in particular in BDL owing to the marked ductular proliferation (Gross et al., 1987; Van de Casteele et al., 2001). Thus, a reduction in arterial flow in rapamycin treated animals is not unexepected in light of the reduction of ductular proliferation. However, hepatic arterial flow was decreased even compared to the sham operated rats suggesting some specific effect of rapamycin on hepatic arterial flow.

Stereological analysis has demonstrated inhibition of two expanding cell lines induced by BDL, namely cholangiocytes and HSC. The antiproliferative activity of rapamycin is well established (Hidalgo and Rowinsky, 2000). Rapamycin is thought to affect the cell cycle through inhibition of mTOR by the FKBP12-rapamycin complex, thereby inhibiting the phosphorylation of $p70^{s6k}$ and of 4E-BP1, impairment of pRb hyperphosphorylation,prevention of p27 down- and of p21 upregulation. p27 and p21 belong

to the kinase inhibitor protein family and are instrumental in the transition from G_1 to S phase. p27 mRNA levels are constant throughout the cell cycle while p27 protein levels are high in non-proliferating cells and low in S phase (Hengst and Reed, 1996). Rapamycin increases p27 protein levels in different cell types (Law et al., 2002; Woltman et al., 2002) thereby inhibiting proliferation. Moreover, fibroblasts and T-lymphocytes from p27 knock-out mice exhibited resistance to the growth-inhibitory effect of rapamycin (Luo et al., 1996).Unchanged p21 mRNA levels in quiescent and proliferating cells have been shown by others (Gaben et al., 2004). p21 protein levels are low in proliferating and high in non-proliferating cells as shown in hepatocytes (Ilyin et al., 2003) and transformed mouse fibroblasts (Gaben et al., 2004). Our observations of p27 and p21 regulation by rapamycin are consistent with these findings: We showed that liver p27 and p21 mRNA steady state levels are not influenced by BDL and that rapamycin treatment significantly increased p27 and decreased p21 protein levels. This might contribute to the inhibition of bile duct proliferation and HSC activation.

The complex of rapamycin and FKBP12 inhibits mTOR (Schmelzle and Hall, 2000). mTOR controls translation via activation through phosphorylation of $p70^{s6k}$ (Shama and Meyuhas, 1996) and inhibition of the eIF4E inhibitor 4E-BP1(Hara et al., 1998). $p70^{s6k}$ is phosphorylated not only by mTOR but also by the phosphoinositide-dependent kinase PDK1 mediating phosphorylation at Thr252 (Alessi et al., 1998). We used an antibody specific for the Ser411 phosphorylation site, a target of mTOR (Isotani et al., 1999). The suppression of $p70^{s6k}$ phosphorylation by rapamycin and, hence, the growth-inhibitory effect has been shown in a variety of different cell types (Jiang et al., 2001). With our findings, we add further evidence that rapamycin inhibits the phosphorylation of $p70^{s6k}$ *in vivo.*

mTOR does not only phosphorylate $p70^{s6k}$ but also 4E-BP1. In a first step, phosphorylation sites Thr37/46 are phosphorylated by mTOR. This is the priming step for the resultant phosphorylation of Ser65 and Thr70 in response to the PI3K or mitogen-activated

protein kinase pathways (Gingras et al., 1998; Gingras et al., 1999). Non-phosphorylated 4E-BP1 inhibits the initiation of translation through the association with eIF-4E. As expected, we did not find a difference in the protein levels of total, non-phosphorylated 4E-BP1 between the different animal groups. To our surprise, neither p-4E-BP1 (Thr37/46) nor p-4E-BP1 (Ser65/Thr70) protein levels were significantly influenced by rapamycin. Moreover, we found significantly more p-4E-BP1 (Ser65/Thr70) in sham-operated rats than in BDL CTR animals. Most of the studies demonstrating inhibition of 4E-BP1 phosphorylation by rapamycin were done in cell culture. Few studies investigated the effect of rapamycin on 4E-BP1 phosphorylation in the intact rat liver. Rapamycin inhibits the amino acid-induced phosphorylation of 4E-BP1 in the perfused rat liver (Shah et al., 1999) and inhibits EGF-, insulin- and cycloheximide-induced phosphorylation of 4E-BP1 in non-regenerating liver (Jiang et al., 2001). In parallel with our findings, these authors found an inhibition of $p70^{s6k}$ phosphorylation by rapamycin. Furthermore, they observed increased levels of p-4E-BP1 (Thr37/46) and p-4E-BP1 (Ser65/Thr70) in the regenerating liver following rapamycin treatment. Thus, in cell culture and in the normal liver rapamycin is capable to inhibit 4E-BP1 phosphorylation. In contrast, in regenerating or cholestatic liver, rapamycin is not affecting 4E-BP1 phosphorylation.

Possibly, 4E-BP1 phosphorylation in the normal liver with low mitogenic activity is controlled by mTOR alone but in the state of injury, a rapamycin-insensitive kinase is induced. The inhibition of at least two other major pathways of cell-cycle progression by rapamycin in the injured liver – p27 up-/p21 downregulation and $p70^{s6k}$ phosphorylation – might serve as an additional stimulus for other kinases to phosphorylate 4E-BP1.

pRb is controlling cell-cycle progression through its repressive effects on the E2Fs transcription factors mediated gene expression (Weintraub et al., 1992). pRb expression *in-vivo* was not shown in normal hepatocytes (Zhao and Zimmermann, 1998), HSC (Abriss et al., 2003) or cholangiocytes (Kang et al., 2002). Consistent with those findings, we were not

able to show pRb in livers of sham-operated, BDL CTR or BDL SIR animals and in long-term serum deprived HEK cells. These results indicate that pRb expression is correlated with the proliferating activity of cells and tissues. We only investigated the pRb expression in the liver 28 days after BDL and therefore cannot exclude that pRb is expressed earlier in the time course of bile duct ligation.

In summary, the present study indicates that rapamycin potently inhibits BDL induced liver fibrosis and bile duct proliferation in rats and thereby ameliorates the development of the hyperdynamic circulation syndrome. We found a decreased production of the pro-fibrogenic and pro-mitogenic cytokines TGF-β1, CTGF and PDGF as well as increased levels of p27, decreased levels of p21 and inhibition of $p70^{s6k}$ phosphorylation while 4E-BP1 phosphorylation seems not to be involved. We conclude, as a working hypothesis, that rapamycin inhibits cellular proliferation through its inhibitory effect on mTOR and that the production of the pro-fibrogenic cytokines is decreased as cellular proliferation is inhibited.

References:

Abriss B, Hollweg G, Gressner AM and Weiskirchen R (2003) Adenoviral-mediated transfer of p53 or retinoblastoma protein blocks cell proliferation and induces apoptosis in culture-activated hepatic stellate cells. *J Hepatol* 38:169-178.

Alessi DR, Kozlowski MT, Weng QP, Morrice N and Avruch J (1998) 3-Phosphoinositide-dependent protein kinase 1 (PDK1) phosphorylates and activates the p70 S6 kinase in vivo and in vitro. *Curr Biol* 8:69-81.

Biecker E, Sagesser H and Reichen J (2004) Vasodilator mRNA levels are increased in the livers of portal hypertensive NO-synthase 3-deficient mice. *Eur J Clin Invest* 34:283-289.

Frazier K, Williams S, Kothapalli D, Klapper H and Grotendorst GR (1996) Stimulation of fibroblast cell growth, matrix production, and granulation tissue formation by connective tissue growth factor. *J Invest Dermatol* 107:404-411.

Friedman SL (1999) Cytokines and fibrogenesis. *Semin Liver Dis* 19:129-140.

Fruman DA, Wood MA, Gjertson CK, Katz HR, Burakoff SJ and Bierer BE (1995) FK506 binding protein 12 mediates sensitivity to both FK506 and rapamycin in murine mast cells. *Eur J Immunol* 25:563-571.

Gaben AM, Saucier C, Bedin M, Barbu V and Mester J (2004) Rapamycin inhibits cdk4 activation, p 21(WAF1/CIP1) expression and G1-phase progression in transformed mouse fibroblasts. *Int J Cancer* 108:200-206.

Gingras AC, Gygi SP, Raught B, Polakiewicz RD, Abraham RT, Hoekstra MF, Aebersold R and Sonenberg N (1999) Regulation of 4E-BP1 phosphorylation: a novel two-step mechanism. *Genes Dev* 13:1422-1437.

Gingras AC, Kennedy SG, O'Leary MA, Sonenberg N and Hay N (1998) 4E-BP1, a repressor of mRNA translation, is phosphorylated and inactivated by the Akt(PKB) signaling pathway. *Genes Dev* 12:502-513.

Grappone C, Pinzani M, Parola M, Pellegrini G, Caligiuri A, DeFranco R, Marra F, Herbst H, Alpini G and Milani S (1999) Expression of platelet-derived growth factor in newly formed cholangiocytes during experimental biliary fibrosis in rats. *J Hepatol* 31:100-109.

Gross JB, Jr., Reichen J, Zeltner TB and Zimmermann A (1987) The evolution of changes in quantitative liver function tests in a rat model of biliary cirrhosis: correlation with morphometric measurement of hepatocyte mass. *Hepatology* 7:457-463.

Groszmann RJ, Vorobioff J and Riley E (1982) Splanchnic hemodynamics in portal-hypertensive rats: measurement with gamma-labeled microspheres. *Am J Physiol* 242:G156-160.

Hara K, Yonezawa K, Weng QP, Kozlowski MT, Belham C and Avruch J (1998) Amino acid sufficiency and mTOR regulate p70 S6 kinase and eIF-4E BP1 through a common effector mechanism. *J Biol Chem* 273:14484-14494.

Hengst L and Reed SI (1996) Translational control of p27Kip1 accumulation during the cell cycle. *Science* 271:1861-1864.

Hidalgo M and Rowinsky EK (2000) The rapamycin-sensitive signal transduction pathway as a target for cancer therapy. *Oncogene* 19:6680-6686.

Ilyin GP, Glaise D, Gilot D, Baffet G and Guguen-Guillouzo C (2003) Regulation and role of p21 and p27 cyclin-dependent kinase inhibitors during hepatocyte differentiation and growth. *Am J Physiol Gastrointest Liver Physiol* 285:G115-127.

Isotani S, Hara K, Tokunaga C, Inoue H, Avruch J and Yonezawa K (1999) Immunopurified mammalian target of rapamycin phosphorylates and activates p70 S6 kinase alpha in vitro. *J Biol Chem* 274:34493-34498.

Jiang YP, Ballou LM and Lin RZ (2001) Rapamycin-insensitive regulation of 4e-BP1 in regenerating rat liver. *J Biol Chem* 276:10943-10951.

Kang YK, Kim WH and Jang JJ (2002) Expression of G1-S modulators (p53, p16, p27, cyclin D1, Rb) and Smad4/Dpc4 in intrahepatic cholangiocarcinoma. *Hum Pathol* 33:877-883.

Khanna A, Plummer M, Bromberek K, Woodliff J and Hariharan S (2002) Immunomodulation in stable renal transplant recipients with concomitant tacrolimus and sirolimus therapy. *Med Immunol* 1:3.

Khanna AK (2000) Mechanism of the combination immunosuppressive effects of rapamycin with either cyclosporine or tacrolimus. *Transplantation* 70:690-694.

Law BK, Chytil A, Dumont N, Hamilton EG, Waltner-Law ME, Aakre ME, Covington C and Moses HL (2002) Rapamycin potentiates transforming growth factor beta-induced growth arrest in nontransformed, oncogene-transformed, and human cancer cells. *Mol Cell Biol* 22:8184-8198.

Lowry O, Rosebrough N, Farr L and Randall R (1951) Protein measurement with the folin phenol reagent. *J Biol Chem* 193:265-275.

Luo Y, Marx SO, Kiyokawa H, Koff A, Massague J and Marks AR (1996) Rapamycin resistance tied to defective regulation of p27Kip1. *Mol Cell Biol* 16:6744-6751.

Morice WG, Wiederrecht G, Brunn GJ, Siekierka JJ and Abraham RT (1993) Rapamycin inhibition of interleukin-2-dependent p33cdk2 and p34cdc2 kinase activation in T lymphocytes. *J Biol Chem* 268:22737-22745.

Moussad EE and Brigstock DR (2000) Connective tissue growth factor: what's in a name? *Mol Genet Metab* 71:276-292.

Nourse J, Firpo E, Flanagan WM, Coats S, Polyak K, Lee MH, Massague J, Crabtree GR and Roberts JM (1994) Interleukin-2-mediated elimination of the p27Kip1 cyclin-dependent kinase inhibitor prevented by rapamycin. *Nature* 372:570-573.

Paradis V, Dargere D, Vidaud M, De Gouville AC, Huet S, Martinez V, Gauthier JM, Ba N, Sobesky R, Ratziu V and Bedossa P (1999) Expression of connective tissue growth factor in experimental rat and human liver fibrosis. *Hepatology* 30:968-976.

Pinzani M, Knauss TC, Pierce GF, Hsieh P, Kenney W, Dubyak GR and Abboud HE (1991) Mitogenic signals for platelet-derived growth factor isoforms in liver fat-storing cells. *Am J Physiol* 260:C485-491.

Sabatini DM, Erdjument-Bromage H, Lui M, Tempst P and Snyder SH (1994) RAFT1: a mammalian protein that binds to FKBP12 in a rapamycin-dependent fashion and is homologous to yeast TORs. *Cell* 78:35-43.

Schmelzle T and Hall MN (2000) TOR, a central controller of cell growth. *Cell* 103:253-262.

Sedlaczek N, Jia JD, Bauer M, Herbst H, Ruehl M, Hahn EG and Schuppan D (2001) Proliferating bile duct epithelial cells are a major source of connective tissue growth factor in rat biliary fibrosis. *Am J Pathol* 158:1239-1244.

Shah OJ, Antonetti DA, Kimball SR and Jefferson LS (1999) Leucine, glutamine, and tyrosine reciprocally modulate the translation initiation factors eIF4F and eIF2B in perfused rat liver. *J Biol Chem* 274:36168-36175.

Shama S and Meyuhas O (1996) The translational cis-regulatory element of mammalian ribosomal protein mRNAs is recognized by the plant translational apparatus. *Eur J Biochem* 236:383-388.

Shibata N, Watanabe T, Okitsu T, Sakaguchi M, Takesue M, Kunieda T, Omoto K, Yamamoto S, Tanaka N and Kobayashi N (2003) Establishment of an immortalized human hepatic stellate cell line to develop antifibrotic therapies. *Cell Transplant* 12:499-507.

Shihab FS, Bennett WM, Yi H, Choi SO and Andoh TF (2004) Sirolimus increases transforming growth factor-beta1 expression and potentiates chronic cyclosporine nephrotoxicity. *Kidney Int* 65:1262-1271.

Tieche S, De Gottardi A, Kappeler A, Shaw S, Sagesser H, Zimmermann A and Reichen J (2001) Overexpression of endothelin-1 in bile duct ligated rats: correlation with activation of hepatic stellate cells and portal pressure. *J Hepatol* 34:38-45.

Van de Casteele M, Sagesser H, Zimmermann H and Reichen J (2001) Characterisation of portal hypertension models by microspheres in anaesthetised rats: a comparison of liver flow. *Pharmacol Ther* 90:35-43.

van der Poel HG (2004) Mammalian target of rapamycin and 3-phosphatidylinositol 3-kinase pathway inhibition enhances growth inhibition of transforming growth factor-beta1 in prostate cancer cells. *J Urol* 172:1333-1337.

Weintraub SJ, Prater CA and Dean DC (1992) Retinoblastoma protein switches the E2F site from positive to negative element. *Nature* 358:259-261.

Wiederrecht GJ, Sabers CJ, Brunn GJ, Martin MM, Dumont FJ and Abraham RT (1995) Mechanism of action of rapamycin: new insights into the regulation of G1-phase progression in eukaryotic cells. *Prog Cell Cycle Res* 1:53-71.

Williams EJ, Gaca MD, Brigstock DR, Arthur MJ and Benyon RC (2000) Increased expression of connective tissue growth factor in fibrotic human liver and in activated hepatic stellate cells. *J Hepatol* 32:754-761.

Woltman AM, Van Der Kooij SW, Coffer PJ, Offringa R, Daha MR and Van Kooten C (2002) Rapamycin specifically interferes with GM-CSF signaling in human dendritic cells leading to apoptosis via increased p27KIP1 expression. *Blood*.

Zhao M and Zimmermann A (1998) Liver cell dysplasia: reactivities for c-met protein, Rb protein, E-cadherin and transforming growth factor-beta 1 in comparison with hepatocellular carcinoma. *Histol Histopathol* 13:657-670.

Zhu J, Wu J, Frizell E, Liu SL, Bashey R, Rubin R, Norton P and Zern MA (1999) Rapamycin inhibits hepatic stellate cell proliferation in vitro and limits fibrogenesis in an in vivo model of liver fibrosis. *Gastroenterology* 117:1198-1204.

Zimmermann H, Blaser H, Zimmermann A and Reichen J (1994) Effect of development on the functional and histological changes induced by bile-duct ligation in the rat. *J Hepatol* 20:231-239.

Footnotes:

This study was supported by the Swiss National Foundation for Scientific Research (grant # 3200-063476 to JR).

JPET Fast Forward. Published on March 15, 2005 as DOI: 10.1124/jpet.104.079616
This article has not been copyedited and formatted. The final version may differ from this version.

Legends to figures

Figure 1. Histological sections of livers from BDL rats with and without rapamycin treatment. CAB-stain of BDL animals without treatment (a) and of BDL animals with rapamycin treatment (b). Arrows indicate bile duct proliferations and connective tissue. Immunohistochemistry for desmin-positve cells (arrows) in BDL animals without treatment (c) and of BDL animals with rapamycin treatment (d). Immunohistochemistry for α-smooth muscle actin (arrows) in BDL animals without treatment (e) and with rapamycin treatment (f). Original magnification 20x

Figure 2. Quantitative real-time PCR of total liver TGF-β1 (a), CTGF (b) and PDGF beta chain (c) mRNA in sham-operated, BDL CTR and BDL SIR rats. Circles represent ΔC_T-values (C_T: the threshold cycle at which an increase in reporter fluorescence above a baseline signal can first be detected; ΔC_T: C_T of mRNA of interest minus C_T of the housekeeping gene GAPDH. Lower ΔC_T-values denote higher mRNA levels) of single animals, the horizontal lines represent the mean mRNA steady-state ΔC_T-values of each group. a: $p=0.001$ comparing TGF-β1 ΔC_T-values of sham-operated and BDL CTR rats. b: $p<0.001$ comparing CTGF ΔC_T-values between all three groups. c: $p<0.01$ comparing PDGF beta chain ΔC_T-values of BDL SIR and BDL CTR rats and $p<0.001$ comparing sham-operated rats with BDL CTR or BDL SIR rats.

Figure 3. TGF-β plasma levels were obtained with an immunoassay. Bars represent the mean values ± S.D. TGF-β plasma levels in the BDL CTR animals were higher ($p<0.02$) than in the BDL SIR animals and higher ($p<0.005$) than in sham-operated animals.
n=6 in all groups.

JPET Fast Forward. Published on March 15, 2005 as DOI: 10.1124/jpet.104.079616
This article has not been copyedited and formatted. The final version may differ from this version.

Figure 4. Quantitative real-time PCR (a), densitometric analysis of Western blots (b) and Western blot (c) of sham-operated, BDL CTR and BDL SIR rats total liver p27 mRNA and protein levels.

a: Circles represent ΔC_T-values of single animals, the horizontal lines represent the mean in p27 mRNA steady-state ΔC_T-values of each group. Differences are not statistically significant.

b: bars represent the mean values ± S.D. of the Western blot band densities x band areas (arbitrary units) of the different treatment groups ($p<0.01$ between all groups).

c: bands show two representative animals of each treatment group.

BDL CTR rats and BDL SIR rats: n=8, sham-operated animals: n=6

Figure 5. Quantitative real-time PCR (a), densitometric analysis of Western blots (b) and Western blot (c) of sham-operated, BDL CTR and BDL SIR rats total liver p21 mRNA and protein levels.

a: Circles represent ΔC_T-values of single animals, the horizontal lines represent the mean in p21 mRNA steady-state ΔC_T-values of each group. Differences are not statistically significant.

b: bars represent the mean values ± S.D. of the Western blot band densities x band areas (arbitrary units) of the different treatment groups ($p<0.01$ between BDL CTR and BDL SIR and BDL CTR and sham operated animals, no difference was obtained when comparing BDL SIR and sham animals).

c: bands show two representative animals of each treatment group.

n=6 in all groups

JPET Fast Forward. Published on March 15, 2005 as DOI: 10.1124/jpet.104.079616
This article has not been copyedited and formatted. The final version may differ from this version.

Figure 6. Densitometric analysis of Western blots (a) and representative Western blots of two animals of each treatment group (b) of total rat liver non-phosphorylated 4E-BP1, phosphorylated 4E-BP1 at Thr37/46 and phosphorylated 4E-BP1 at Ser65/Thr70.
Bars represent the mean values ± S.D. of the Western blot band densities x band areas (arbitrary units) of the different treatment groups. There are no statistically significant differences between the treatment groups for non-phosphorylated 4E-BP1 and phosphorylated 4E-BP1 (Thr37/46). Only the difference of phosphorylated 4E-BP1 (Ser65/Thr70) in sham vs. BDL CTR rats is significant ($p<0.01$).
BDL CTR and BDL SIR rats: n=8, sham-operated animals: n=6

Figure 7. Densitometric analysis of Western blots (a) and representative Western blots of two animals of each treatment group (b) of rat total liver non-phosphorylated $p70^{s6k}$ and phosphorylated $p70^{s6k}$.
Bars represent the mean values ± S.D. of the Western blot band densities x band areas (arbitrary units) of the different treatment groups. There are no statistically significant differences between the treatment groups for non-phosphorylated $p70^{s6k}$. p-$p70^{s6k}$: $p<0.001$ comparing BDL CTR rats with BDL SIR rats, $p<0.01$ comparing sham-operated animals with BDL CTR rats and BDL SIR rats.
BDL CTR and BDL SIR rats: n=8, sham-operated animals: n=6

Figure 8. Western blot of pRb in rat liver. Representative blots of two animals of each treatment group are shown. Lysates of cultured human embryonic kidney cells (HEK), harvested in the exponential growing phase or kept for 96 h without serum as well as normal rat cholangiocytes (NRC) harvested in the exponential growing phase or kept for 24 h without serum served as controls.

JPET Fast Forward. Published on March 15, 2005 as DOI: 10.1124/jpet.104.079616
This article has not been copyedited and formatted. The final version may differ from this version.

Table 1. Sequences, concentrations and Genebank accession numbers of the primers and probes.

Gene	Accession number	Primer/Probe sequence (Forward / Reverse / Probe)	Primer/Probe concentration (nmol/l)
PDGF-B chain	Z14117.1	CCGCTCCTTTGATGACCTTC	300
		GCTCAGCCCCATCTTCGTC	300
		CGCCTGCTGCACAGAGACTCCG	100
TGF-β1	X52498.1	GTCCCAAACGTCGAGGTGAC	300
		GCCATGAGGAGCAGGAAGG	300
		TGGGCACCATCCATGACATGAACC	100
CTGF	NM_022266	TCTCTTCTGCGACTTCGGCT	900
		CATCTTTGGCAGTGCACACG	900
		CCCCGCCAACCGCAAGATTG	200
p27	D83792.1	CTTCCGCCTGCAGAAACCT	300
		CTTCTCCAAGTCCCGGGTTAG	900
		TTCGGCCCGGTCAATCATGAAGA	200

JPET Fast Forward. Published on March 15, 2005 as DOI: 10.1124/jpet.104.079616
This article has not been copyedited and formatted. The final version may differ from this version.

Table 2. Data and conditions of primary and secondary antibodies used for Western blotting.

1. Antibody anti-	SDS-PAGE conditions	Dilution 1. Antibody	2. Antibody	Dilution 2. Antibody
PRb	7.5 %	1:2500	goat-anti-mouse	1:15000
p27	15%	1:1000	donkey-anti-rabbit	1:64000
$p70^{s6k}$	10%	1:100	rabbit-anti-goat	1:50000
p-$p70^{s6k}$ (Ser411)	10%	1:100	goat-anti-mouse	1:15000
4E-BP1	15%	1:2000	rabbit-anti-goat	1:50000
p-4E-BP1 (Ser65/Thr70)	15%	1:200	donkey-anti-rabbit	1:64000
p-4E-BP1 (Thr37/46)	15%	1:200	donkey-anti-rabbit	1:64000
p21	12%	1:200	goat-anti-mouse	1:7500

Anti-pRb and p21were obtained from BD Transduction Laboratories, Lexington, KY, USA. Anti-p-4E-BP1 (Thr37/46) was from Cell signaling technology, MA, USA. The remaining primary antibodies were from Santa-Cruz Biotechnology, CA, USA. All secondary antibodies were obtained from Pierce Biotechnology, IL, USA.

JPET Fast Forward. Published on March 15, 2005 as DOI: 10.1124/jpet.104.079616
This article has not been copyedited and formatted. The final version may differ from this version.

Table 3. Animal characteristics.

Treatment group	Body weight* (g)	Liver weight§ (g)	Spleen weight# (g)	AST+ (U/l)	Bilirubin** (µmol/l)	Bile acids++ (µmol/l)
Sham (n=6)	303.8 ± 45	12.9 ± 2.9	0.8 ± 0.1	78.3 ± 8.7	84.1 ± 23.2	14.0 ± 8.5
BDL SIR (n=8)	335.9 ± 28	20.3 ± 3.4	0.9 ± 0.1	92.6 ± 27.3	423.2 ± 167.0	58.2 ± 37.7
BDL CTR (n=8)	362.1 ± 43.8	27 ± 5.8	2.3 ± 0.7	271.4 ± 79.0	1296.8 ± 868.1	279.5 ± 108.5

Animal characteristics of sham-operated rats, BDL CTR rats and BDL SIR rats. *: $p < 0.05$ comparing BDL CTR rats with sham-operated rats. §: $p < 0.01$ between all groups. #: $p < 0.001$ comparing BDL SIR rats with BDL CTR rats and between BDL CTR rats and sham-operated animals. +: $p < 0.001$ comparing BDL CTR with BDL SIR and sham-operated rats. **: $p < 0.01$ comparing BDL CTR with BDL SIR and sham-operated rats. ++: $p < 0.001$ comparing BDL CTR with BDL SIR and sham-operated rats.

JPET Fast Forward. Published on March 15, 2005 as DOI: 10.1124/jpet.104.079616
This article has not been copyedited and formatted. The final version may differ from this version.

Table 4. Hemodynamic parameters.

Treatment group	MAP (mmHg)	PVP * (mmHg)	Cardiac output§ (ml/min/100g)	Hepatic artery blood flow # (ml/min/g)	Portal vein blood flow + (ml/min/g)
Sham (n=6)	120 ± 13	6.7 ± 1.4	26.1 ± 4.0	0.7 ± 0.2	3 ± 0.5
BDL SIR (n=8)	112 ± 15	11.8 ± 1	29 ± 5.3	0.3 ± 0.1	2.7 ± 1
BDL CTR (n=8)	104 ± 10	15 ± 2.6	33 ± 4.7	0.7 ± 0.2	1.5 ± 0.4

Hemodynamic parameters of sham-operated rats, BDL CTR rats and BDL SIR rats. *: $p < 0.01$ between all three groups. §: $p < 0.05$ comparing sham rats with BDL CTR rats. #: $p < 0.001$ comparing BDL SIR rats with sham and BDL CTR rats. +: $p < 0.01$ comparing BDL CTR rats with BDL SIR rats and $p < 0.001$ comparing BDL CTR rats with sham-operated animals.

JPET Fast Forward. Published on March 15, 2005 as DOI: 10.1124/jpet.104.079616
This article has not been copyedited and formatted. The final version may differ from this version.

Table 5. Morphometric analysis of liver sections.

Group	Volume fraction (%)	
	BDL CTR, n=7	BDL SIR, n=11
Hepatocytes	55.4 ± 12.2	76.2 ± 3.1*
Connective tissue	10.4 ± 4.4	5.0 ± 1.8*
Bile duct epithelial cells	18.3 ± 7.5	4.5 ± 3.7*
Desmin positive cells	14.5 ± 3.4	7.4 ± 2.7*
Actin positive cells	11.1 ± 7.6	3.1 ± 4.2*
Actin/desmin positive cells	0.71 ± 0.37	0.34 ± 0.4*

Results of morphometric analysis of liver sections of BDL rats with and without rapamycin treatment. *:Differences between BDL rapamycin treated and non-treated rats are statistically significant ($p<0.05$)

JPET Fast Forward. Published on March 15, 2005 as DOI: 10.1124/jpet.104.079616
This article has not been copyedited and formatted. The final version may differ from this version.

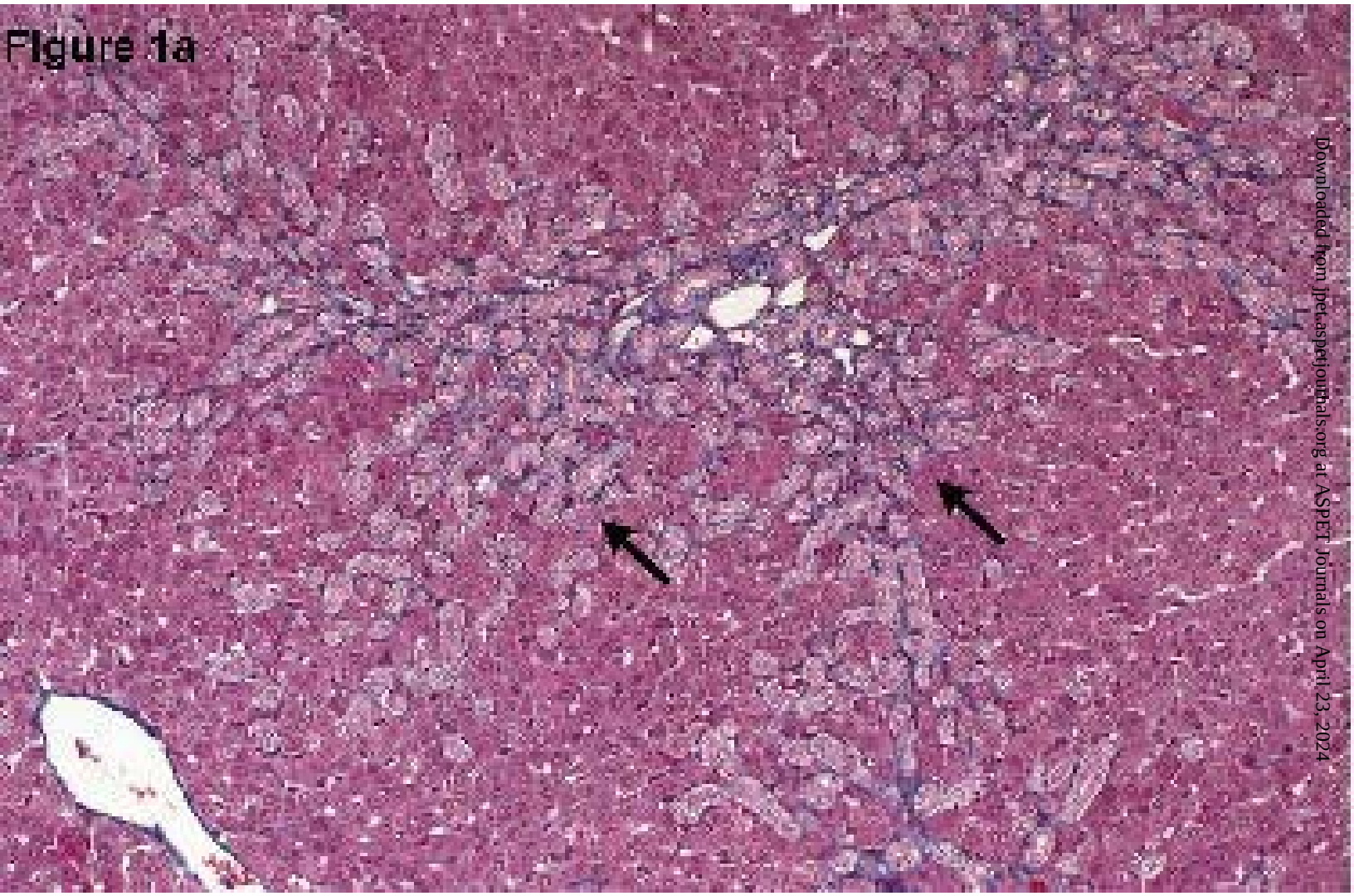

JPET Fast Forward. Published on March 15, 2005 as DOI: 10.1124/jpet.104.079616
This article has not been copyedited and formatted. The final version may differ from this version.

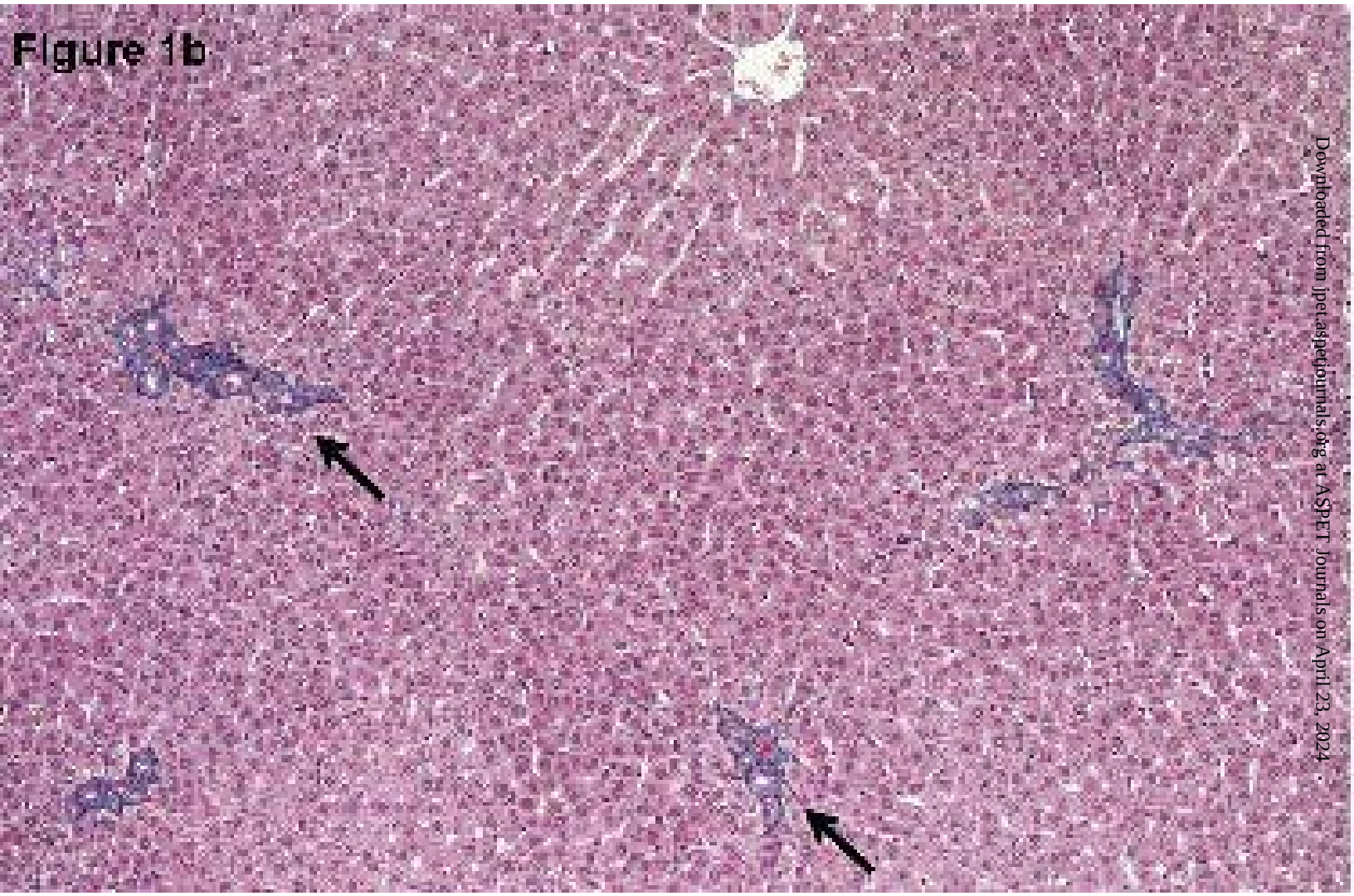

JPET Fast Forward. Published on March 15, 2005 as DOI: 10.1124/jpet.104.079616
This article has not been copyedited and formatted. The final version may differ from this version.

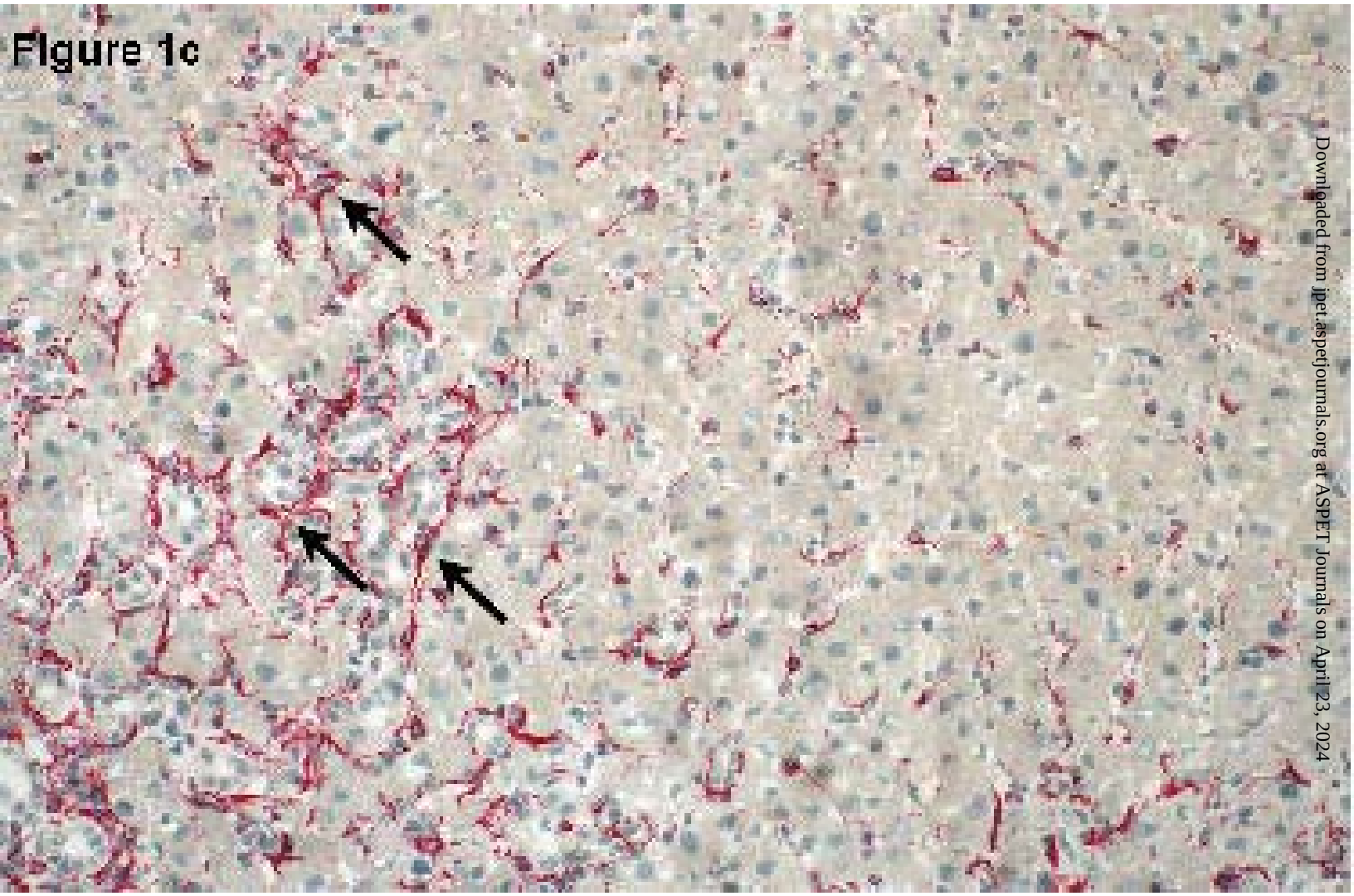

JPET Fast Forward. Published on March 15, 2005 as DOI: 10.1124/jpet.104.079616
This article has not been copyedited and formatted. The final version may differ from this version.

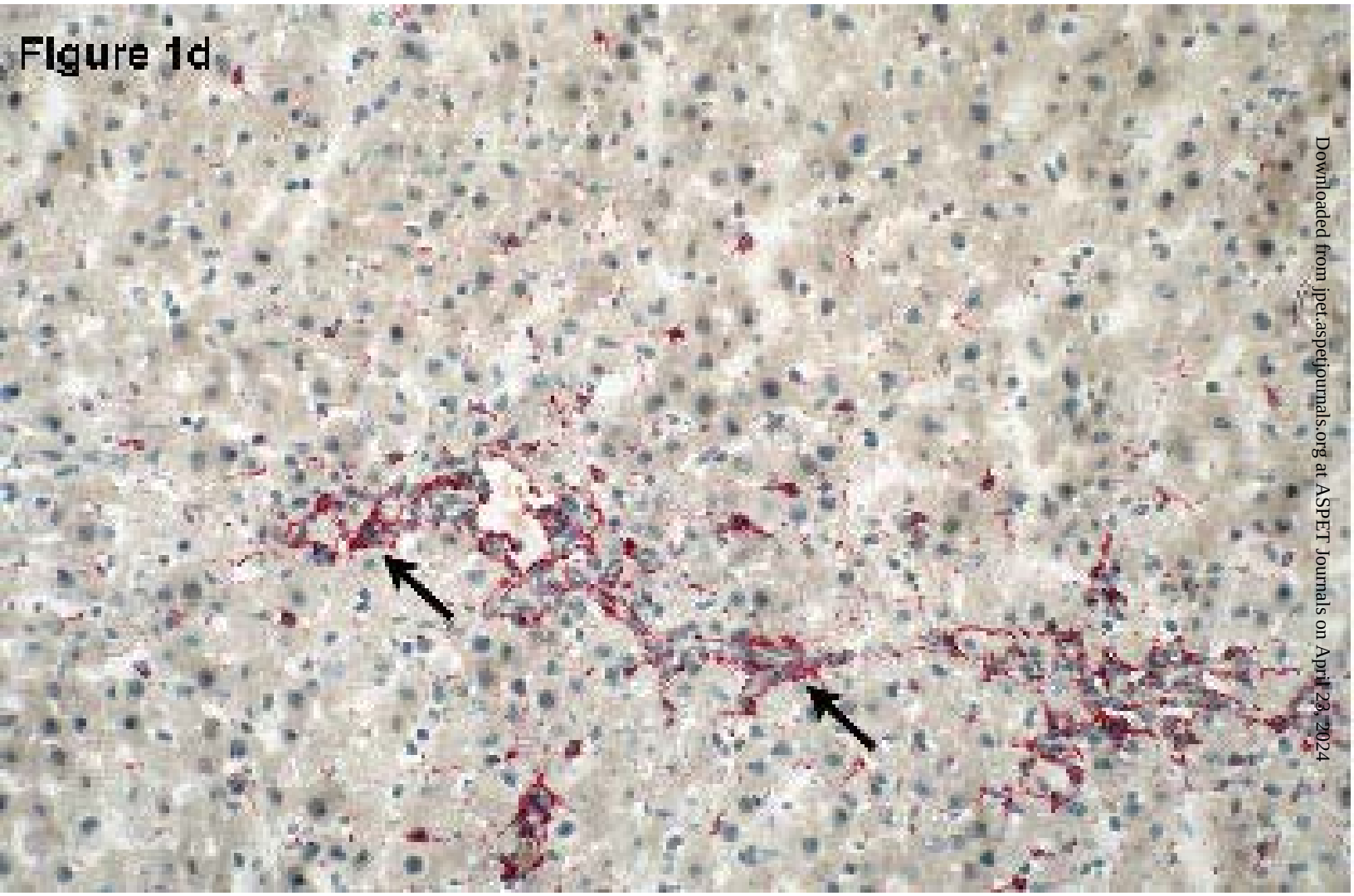

JPET Fast Forward. Published on March 15, 2005 as DOI: 10.1124/jpet.104.079616
This article has not been copyedited and formatted. The final version may differ from this version.

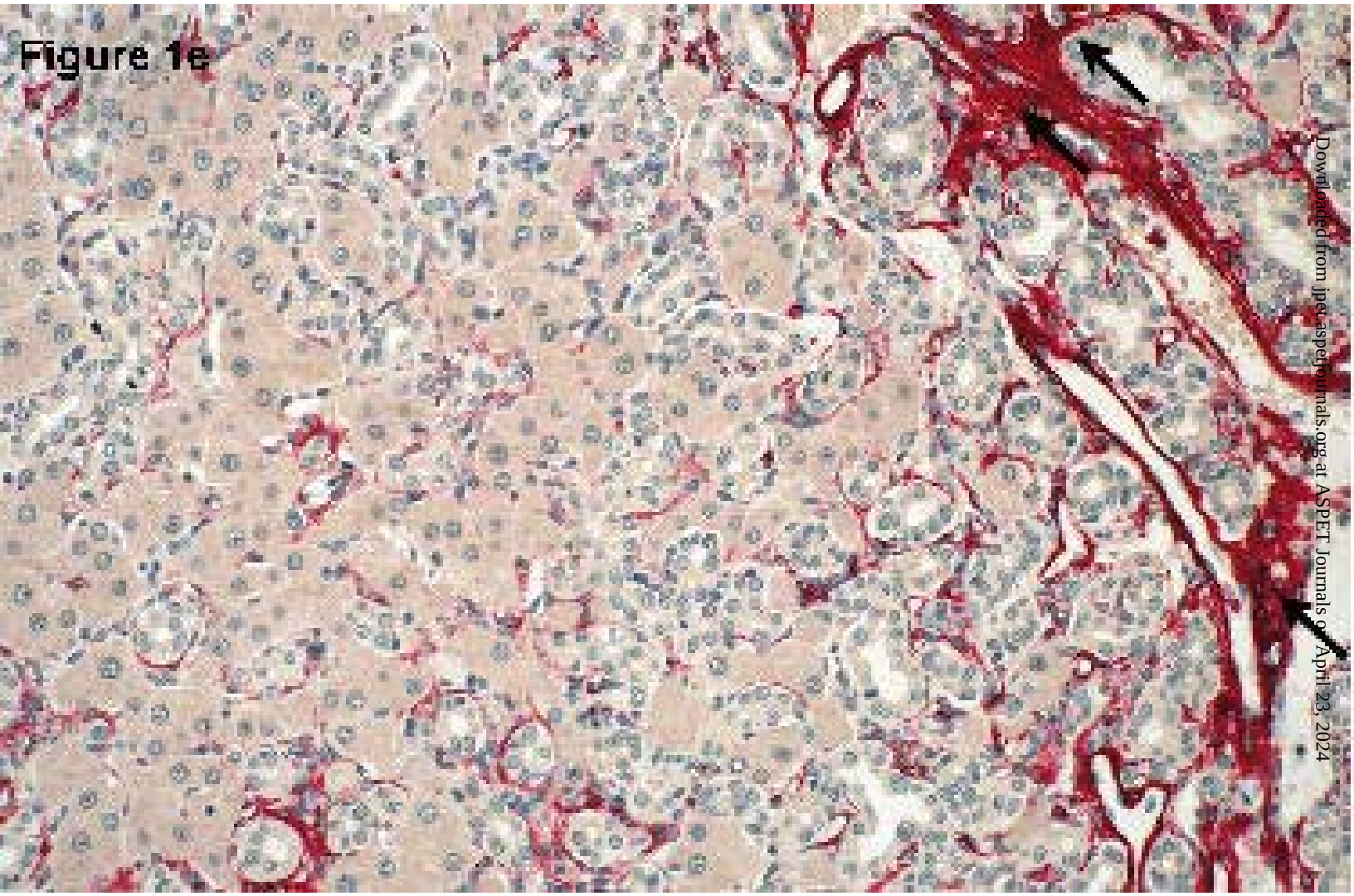

JPET Fast Forward. Published on March 15, 2005 as DOI: 10.1124/jpet.104.079616
This article has not been copyedited and formatted. The final version may differ from this version.

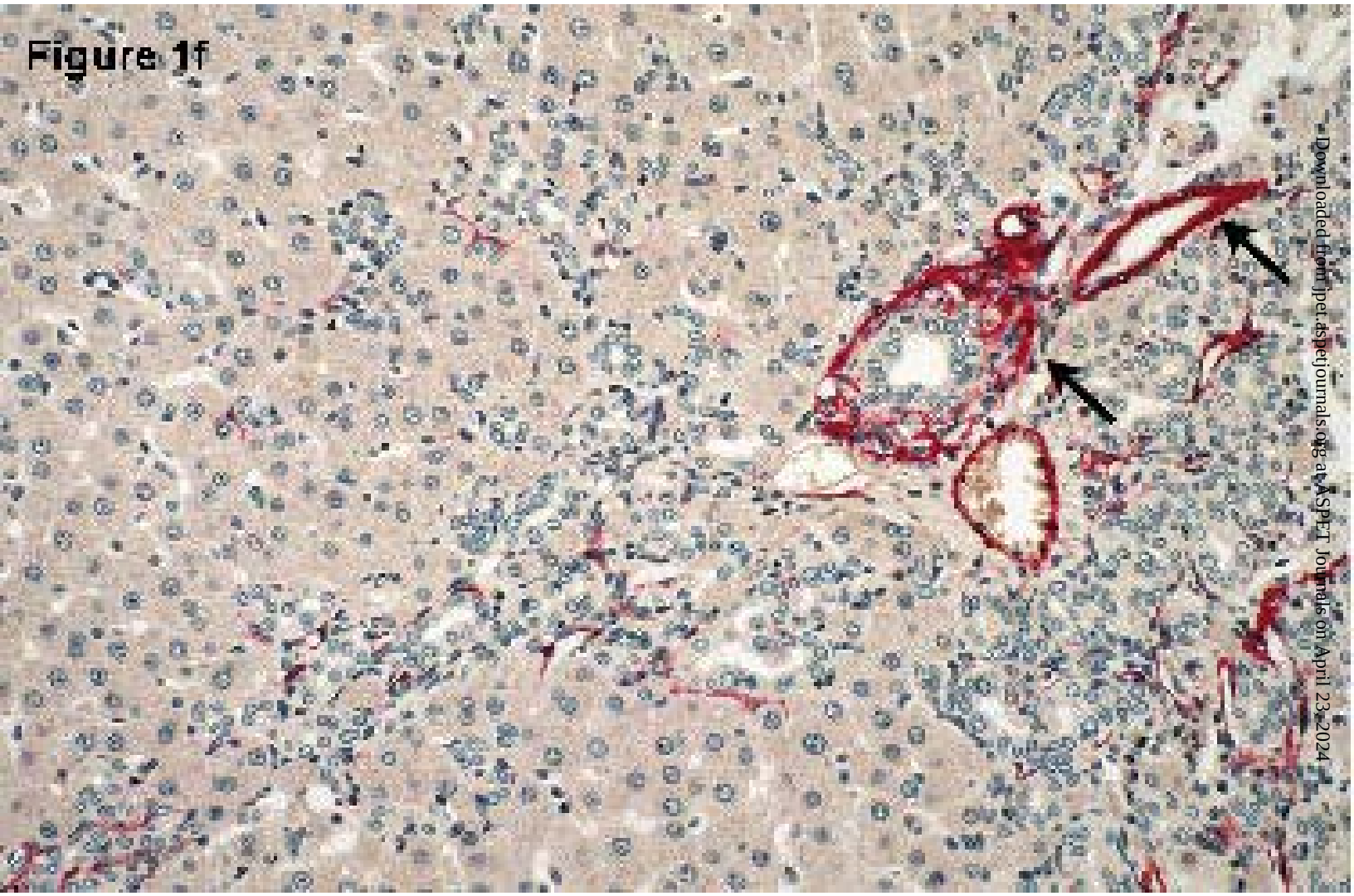

Figure 2

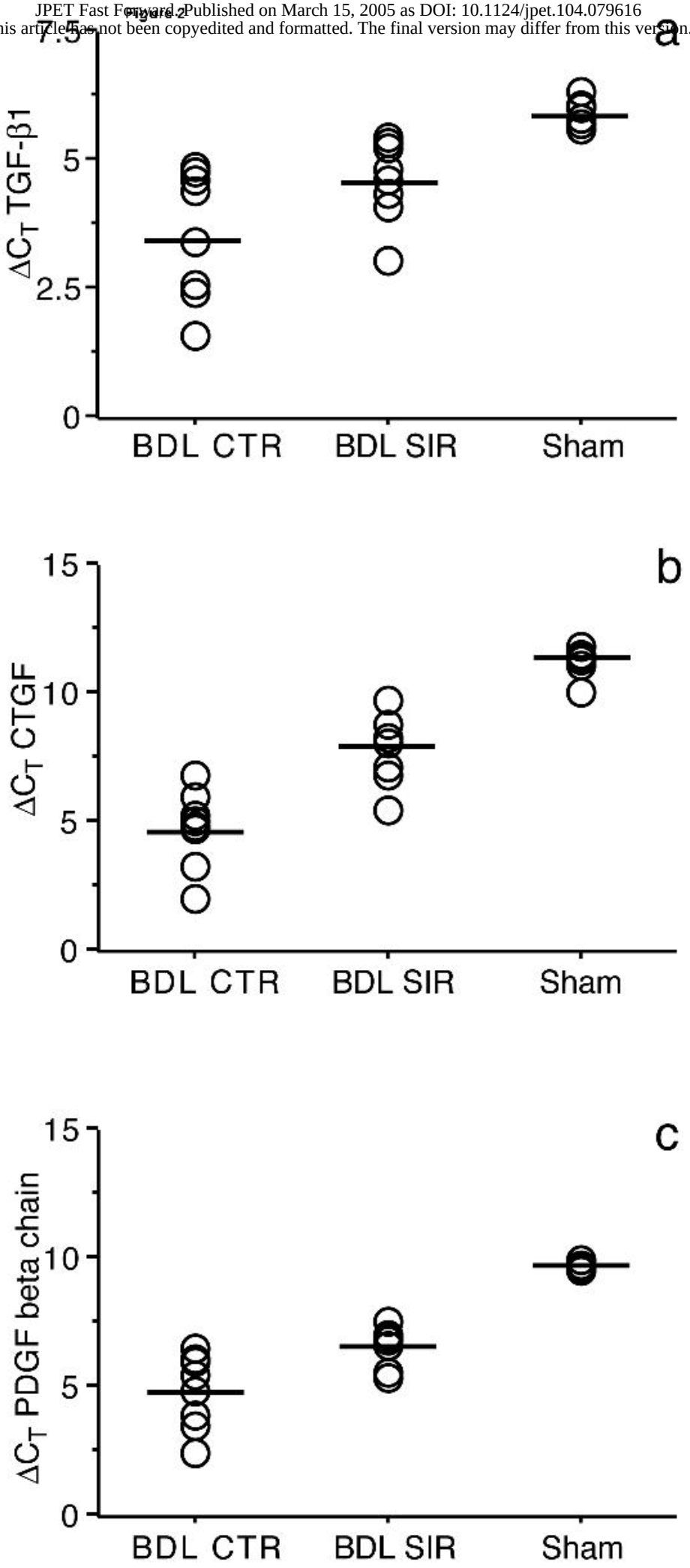

JPET Fast Forward. Published on March 15, 2005 as DOI: 10.1124/jpet.104.079616
This article has not been copyedited and formatted. The final version may differ from this version.

Figure 3

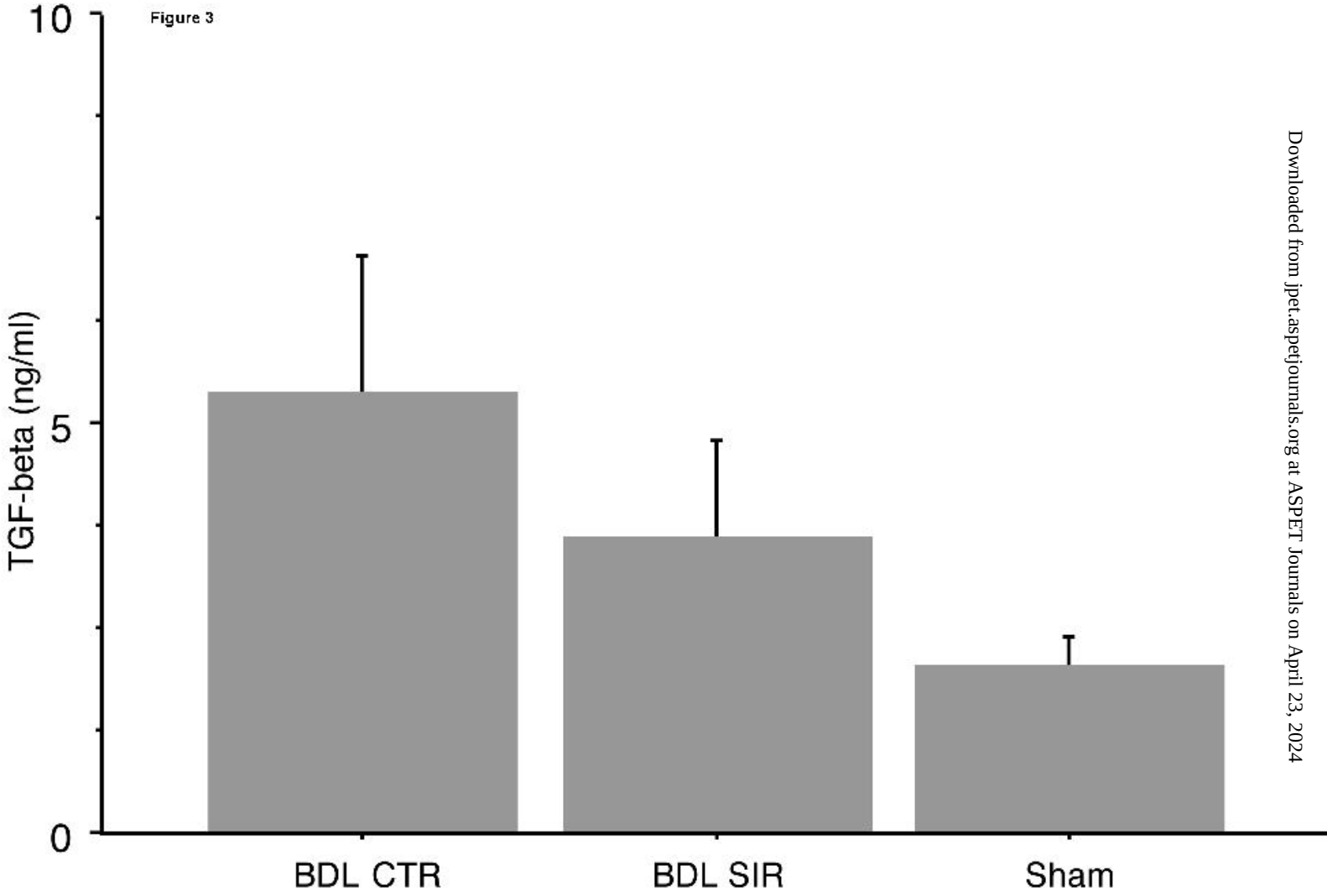

JPET Fast Forward. Published on March 15, 2005 as DOI: 10.1124/jpet.104.079616
This article has not been copyedited and formatted. The final version may differ from this version.

Figure 4

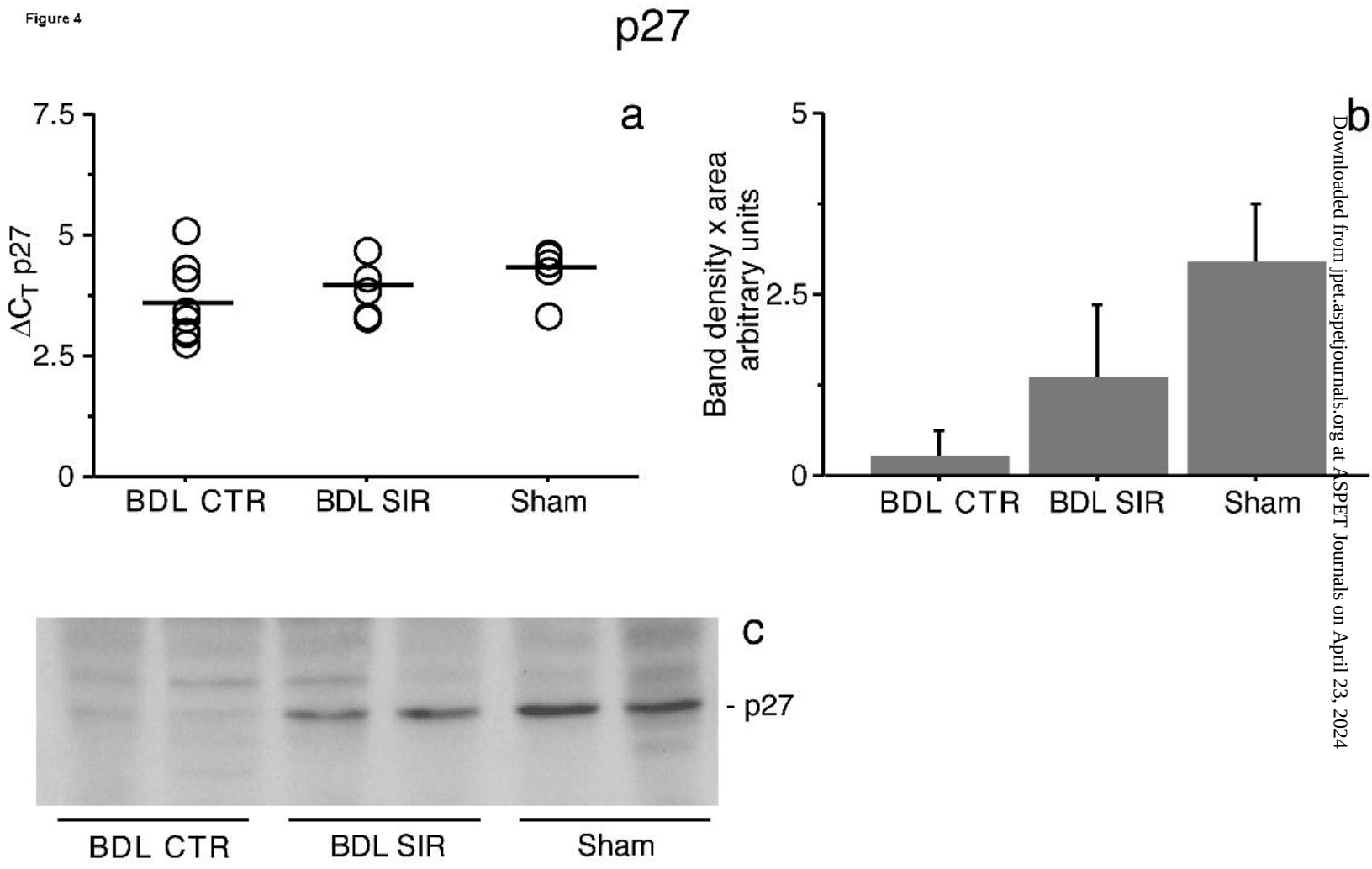

JPET Fast Forward. Published on March 15, 2005 as DOI: 10.1124/jpet.104.079616
This article has not been copyedited and formatted. The final version may differ from this version.

Figure 5

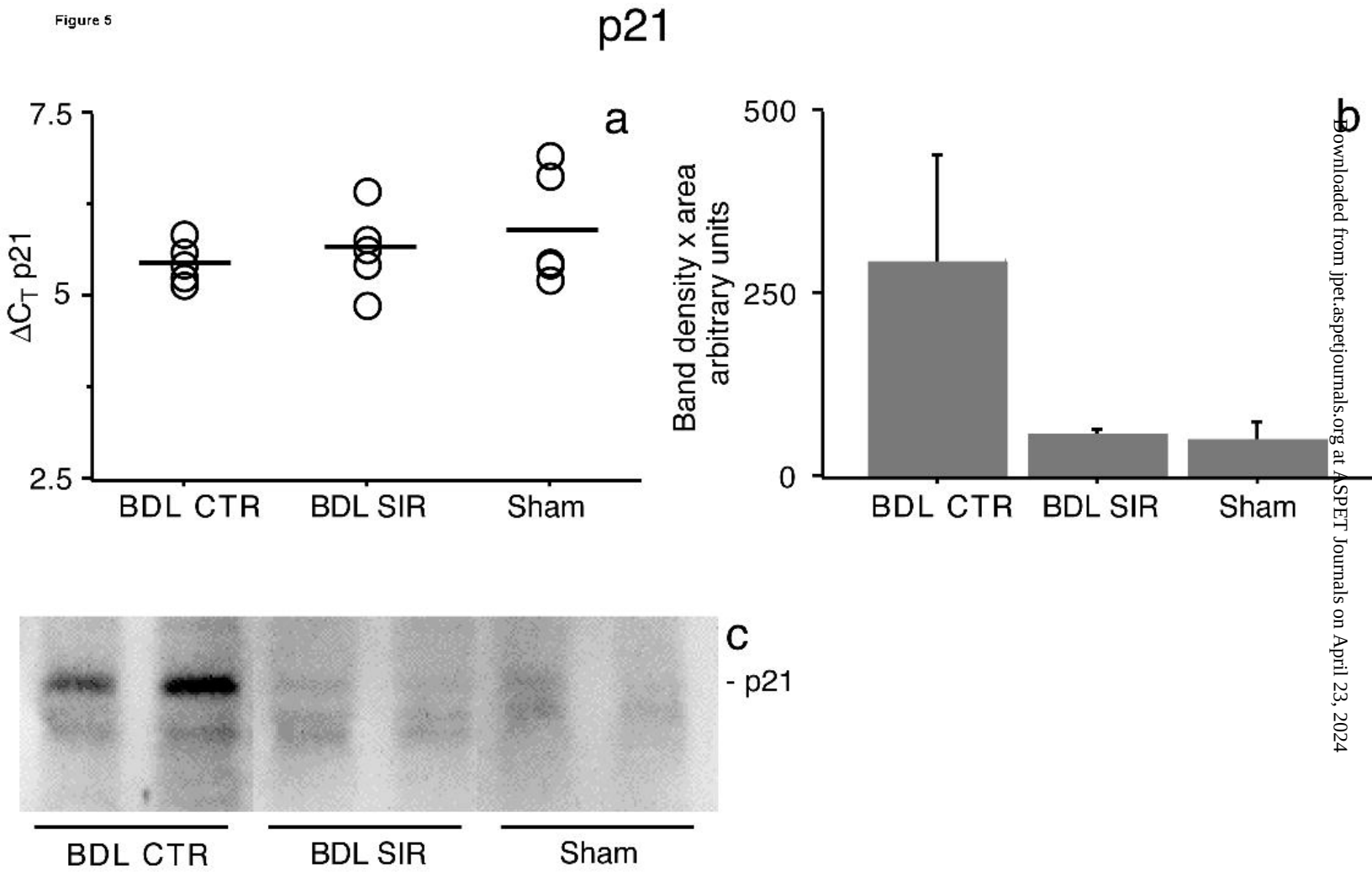

JPET Fast Forward. Published on March 15, 2005 as DOI: 10.1124/jpet.104.079616
This article has not been copyedited and formatted. The final version may differ from this version.

Figure 6

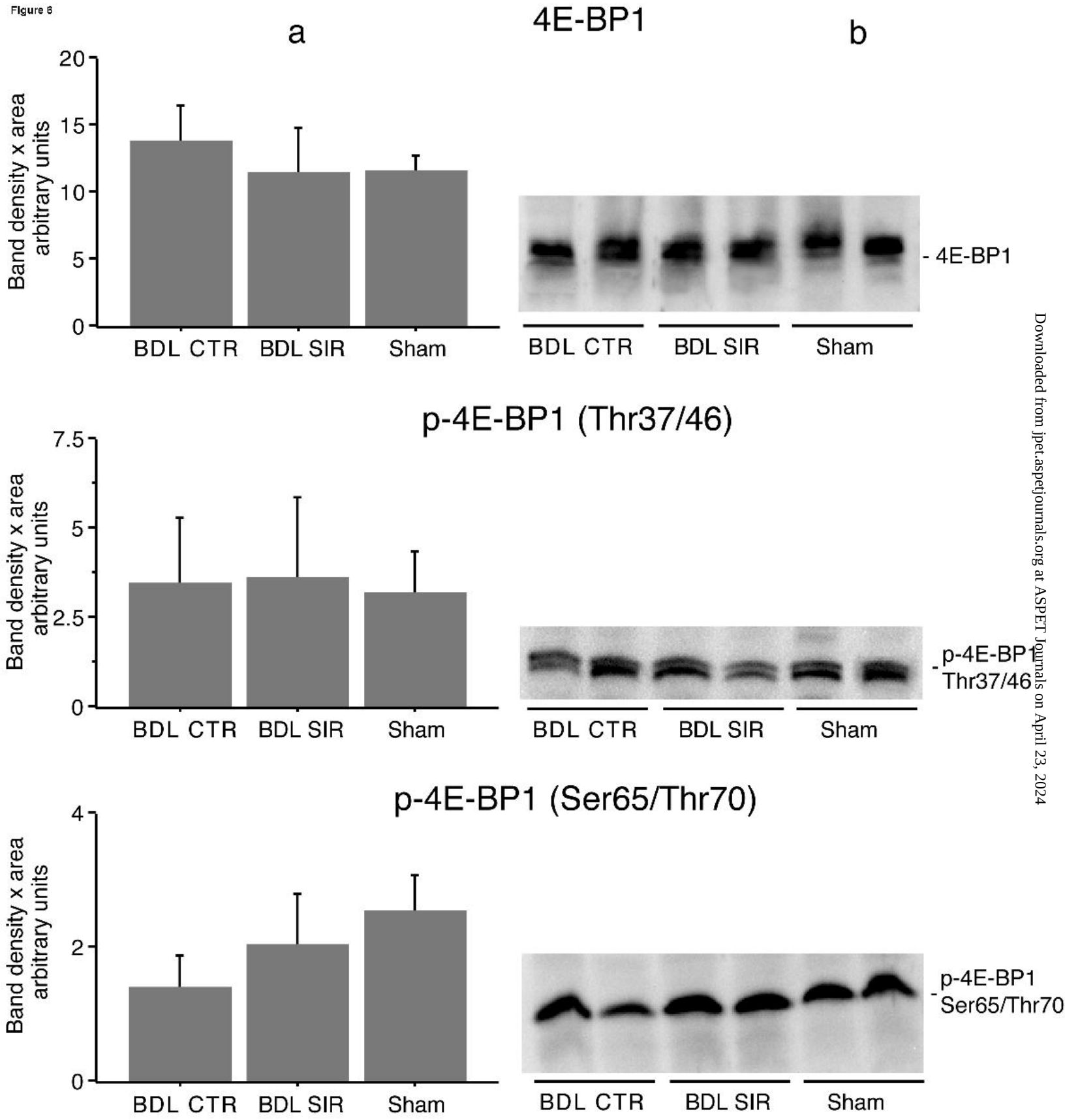

JPET Fast Forward. Published on March 15, 2005 as DOI: 10.1124/jpet.104.079616
This article has not been copyedited and formatted. The final version may differ from this version.

Figure 7

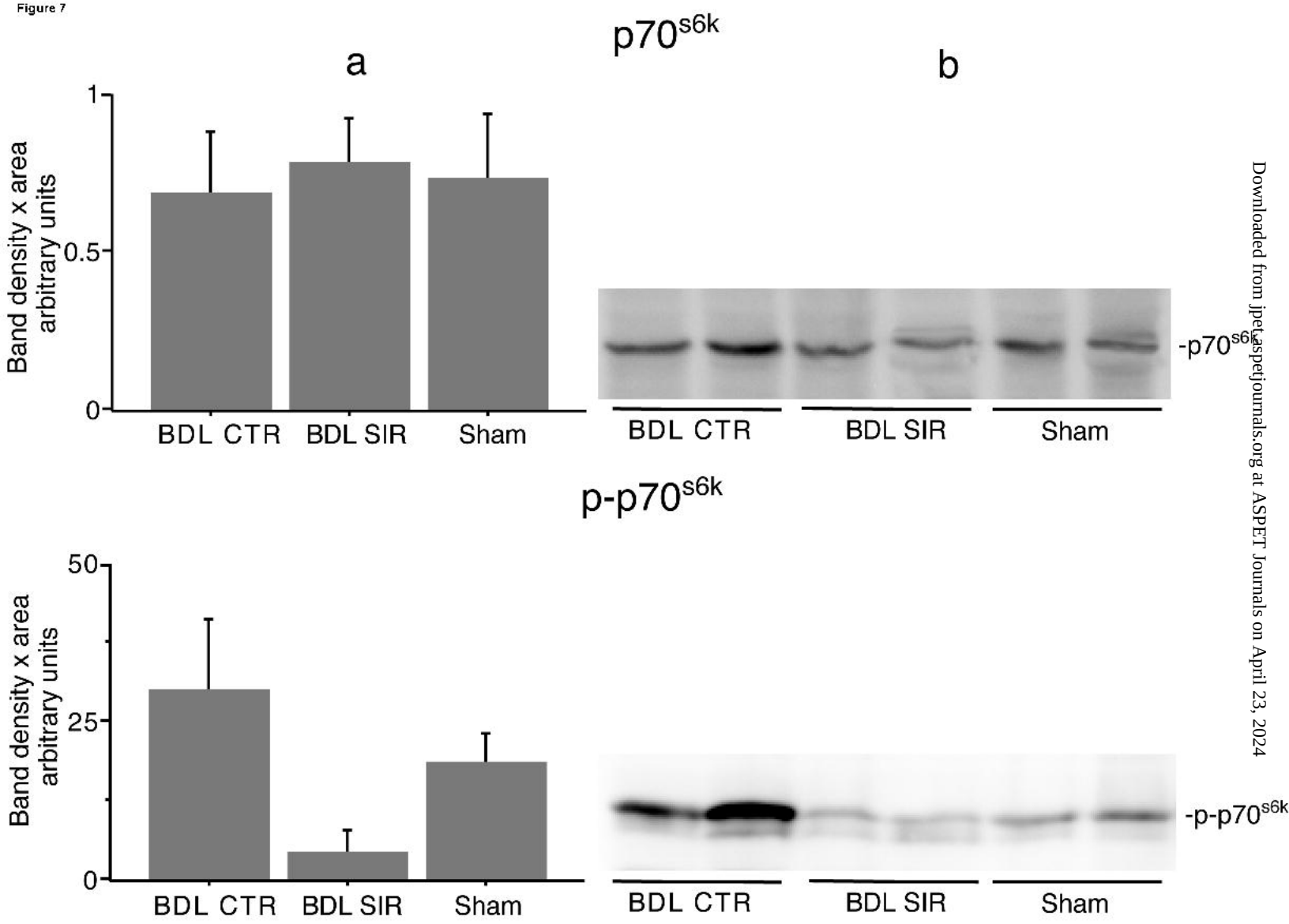

JPET Fast Forward. Published on March 15, 2005 as DOI: 10.1124/jpet.104.079616
This article has not been copyedited and formatted. The final version may differ from this version.

Figure 8